

Oxidation Behavior of Y_2O_3 and Er_2O_3 -doped- α/β -SiAlON Ceramics

*Ali Çelik

Bilecik Şeyh Edebali University Metallurgical and Materials Engineering Department, Bilecik/Turkey,
ali.celik@bilecik.edu.tr, 

Research Paper

Arrival Date: 21.01.2019

Accepted Date: 07.05.2019

Abstract

SiAlON ceramics are successfully utilized in applications such as refractories used for metal melting and cutting tools for high speed machining of metals in which high temperature properties are important. As being one of the main indication of high temperature resistance for such applications, oxidation resistance of this materials are affected by microstructural features, type and amount of the rare-earth (RE) elements in α -SiAlON and grain boundary phase (GBP). In this study, oxidation behavior of α/β -SiAlON ceramics prepared by Er_2O_3 as well as Y_2O_3 , which is one of the most widely used RE-oxide in commercial SiAlON compositions, was investigated comparatively. A slight difference was observed in oxidation resistance of Er_2O_3 and Y_2O_3 containing SiAlON ceramics due to their slightly different crystallinity of GBPs.

Keywords: Oxidation, SiAlON, Rare-earth elements

Y_2O_3 ve Er_2O_3 -katkılı α/β -SiAlON Seramiklerinin Oksidasyon Davranışları

*Ali Çelik

Bilecik Şeyh Edebali Üniversitesi Metalurji ve Malzeme Mühendisliği Bölümü, Bilecik/Türkiye,
ali.celik@bilecik.edu.tr, 

Öz

SiAlON seramikleri metal ergitme işleminde kullanılan refrakterler ve metallerin yüksek kesme hızlarında talaşlı imalatında kullanılan kesici takımlar gibi yüksek sıcaklık özelliklerinin ön planda olduğu uygulamalarda başarıyla kullanılan malzemelerdir. Bu malzemelerin oksidasyon ve korozyon direnci gibi yüksek sıcaklık özellikleri ise mikroyapısal özellikleri, faz özellikleri ve kullanılan nadir toprak (RE) elementleri ile belirlenmektedir. Bu çalışmada ve sağladığı yüksek oksidasyon direnci ile SiAlON seramiklerinin üretiminde en yaygın kullanılan nadir toprak elementi oksitlerinden bir tanesi olan Y_2O_3 ile birlikte önemli bir potansiyele sahip olan Er_2O_3 ilaveleri kullanılarak hazırlanan α/β -SiAlON seramiklerinin kıyaslamalı oksidasyon davranışları incelenmiştir. Oksidasyon direnci açısından her iki ilavenin benzer özelliklere sahip olduğu, farklılığın ise tane sınırı fazlarının kristalizasyon derecelerinden kaynaklandığı bulunmuştur.

Anahtar Kelimeler: Oksidasyon, SiAlON, Nadir toprak elementleri

1. INTRODUCTION

SiAlON ceramics are one of the most attractive engineering materials for various applications due to their high hardness, fracture toughness, thermal shock and corrosion resistance. The possibility to obtain all these properties in a single material by just altering the types and amounts of α -SiAlON, β -SiAlON and GBP makes this material suitable for many

challenging applications. α -SiAlON phase is 40% harder than β -SiAlON, which has higher fracture toughness due to its elongated grain shape [1-3]. Since both high fracture toughness and hardness are required for many structural applications, in-situ α/β -SiAlON composites are more suitable in comparison to the single phase monolithic SiAlONs. Cutting tools for high speed machining of gray cast iron and superalloys are the most well-known

*Corresponding Author: Bilecik Şeyh Edebali University Metallurgical and Materials Engineering Department, Bilecik/Turkey,
ali.celik@bilecik.edu.tr

application and crystallization of GBP as well as combination of hardness and toughness provided by α and β -SiAlON phases are critically important for high temperature resistance for SiAlON based cutting tools [4].

The oxidation is one of the main problems for not only SiAlON ceramics but also the other Si-based synthetic ceramic materials such as SiC, Si₃N₄, etc. due to their thermodynamic instability in open atmosphere at high temperatures. Çelik et al. [5] manufactured SiAlON based ceramic milling tools and tested them on high speed milling of superalloys. According to author's conclusions on test results, the cutting zone temperature exceeded to 1000°C, and oxidation and other diffusion processes became dominant at given test conditions. Therefore, the investigation of effective parameters on the oxidation behavior of SiAlON ceramics was considered as an important subject for improving high temperature properties of these ceramics and subjected to many researches in the literature. For β -SiAlON phase, z value in the general formula of Si_{6-z}Al_zO_zN_{8-z}, indicating the solubility of Al and O atoms in crystal structure of β -Si₃N₄, is an effective parameter on the formation of the oxide crystal products as the result of oxidation reactions since it affects the amount and viscosity of the GBP [6,7]. On the other hand, the RE element oxides are highly effective on the nature of oxidation resistance of α -SiAlON phase. Yu et al. [8] investigated the oxidation behavior of α -SiAlON ceramics doped with Yb, Y, Nd, Ca and Li-oxides between 1000-1300°C and reported that the oxidation resistance increased in the order of Li, Ca, Nd, Y and Yb. They concluded that the refractoriness of the oxidation products on the surface and crystallinity of GBP, which are strongly dependent on type of the RE used, play an important role on the oxidation resistance. In a similar work, Corapcıoğlu and Kurama [9] examined the oxidation resistance of Y and Sm single doped and Y/Sm multi-doped α -SiAlON ceramics at the temperatures between 1300-1450°C and found the viscosity of GBP as an effective parameter on oxidation resistance of the ceramics. It was reported by the authors that using of both Sm and Y as multi dopant resulted in a slight increase in oxidation resistance in comparison to the single doped SiAlON compositions. Nordberg and et al. [10] utilized Y, Yb, Sm and Nd in α -SiAlON compositions and investigated the oxidation behavior of these ceramics. Oxidation resistance of ceramics doped with Nd and Sm was found lower than that of Y and Yb doped counter-parts due to lack of N-rich melilite phase crystallization at the grain boundaries of Sm and Nd doped SiAlONs.

In this study, comparative oxidation behavior of Er₂O₃ and Y₂O₃-doped α/β -SiAlON ceramic at 1250-1550°C was investigated by a scanning electron microscope (SEM) and an x-ray diffractometer (XRD). The weight change of the SiAlON ceramics due to oxidation reactions was also analyzed.

2. MATERIALS AND METHODS

2.1. Production of SiAlON samples

α/β -SiAlON compositions doped with Y₂O₃ and Er₂O₃, labelled as Y-S and Er-Si, respectively, were designed as the ratio of α/β is 25/75% and z value of β -SiAlON (Si_{6-z}Al_zO_zN_{8-z}) is 0.2. α -Si₃N₄ powder, as the main component of SiAlON compositions, and Al₂O₃ AlN, Y₂O₃ and Er₂O₃ powders, which provides formation of liquid phase and stabilization of α -SiAlON phase during sintering were charged to the chamber of an attritory mill. The powders were milled for 2 hours in aqueous medium in the presence of Si₃N₄ milling balls with a diameter of 3 mm for an efficient milling process. After mixing the slurries with organic pressing additives in a separate chamber for 30 min., spray drying (LTC-2 Nubilosa) was performed to obtain granules with high flowability. The average particle size of the granules with a moisture content of ~1 wt.% was 100 μ m. In shaping step, SiAlON granules were transferred to a cylindrical flexible polyurethane mold of cold isostatic press (MSE-CIP200) and then 200 MPa isostatic pressing pressure was applied to the mold setup in order to obtain SiAlON compacts with a green density of ~55% of theoretical density. Subsequent to a binder removal step performed at ~600°C prior to sintering, the green cylindrical compacts were placed to the chamber of gas pressure sintering (GPS) furnace (FCT-FPW180/2200). The samples were densified to >99,8 % of theoretical density at a maximum temperature and N₂ gas pressure of 1900°C and 100 bar, respectively.

2.2. Oxidation tests and characterization

After sintering, cylindrical SiAlON samples were cut into pellets with a thickness of 5 mm and top and bottom grinding of the sintered pellets was performed by a polymer bonded diamond wheel (average diameter of diamond particles is 120 μ m). Then, the pellets were oxidized at 4 different temperatures (1250, 1350, 1450 and 1550°C) with a soaking time of 2 hours under normal atmospheric conditions. Before and after each oxidation tests, the samples were weight with a four-digit scale in order to find the weight change depending on the oxidation reactions. The phases inside as-sintered samples and formed on the surface of oxidized samples were identified by an x-ray diffractometer (XRD) (Rigaku-Miniflex). From the XRD spectrum, intensity of the peaks of α -SiAlON phase at $2\theta=34.5$ ve 35.3° and of β -SiAlON phase at $2\theta=33.7$ ve 36° were used to calculate the α/β -SiAlON phase ratio by following equation:

$$\frac{I_\beta}{I_\beta + I_\alpha} = \frac{1}{1 + K [(1/w_\beta) - 1]} \quad (1)$$

where I_β and I_α are the x-ray intensities of β and α -SiAlON peaks respectively, K is constant (0.518 for the peaks diffracted by (101) plane of β -SiAlON and (102) plane of α -SiAlON and 0.544 for the peaks diffracted by (210) plane of β -SiAlON and (210) plane of α -SiAlON), w_β is the

concentration of β -SiAlON phase in volume %. z value of β -SiAlON in general formula of $\text{Si}_{6-z}\text{Al}_z\text{O}_z\text{N}_{8-z}$ was determined by the shifts of corresponding peaks due to solubility of Al_2O_3 in Si_3N_4 crystal lattice and calculated by taking the average of z_a and z_c which are given in Equations 2 and 3 as follow:

$$z_a = \frac{a - 7.6044}{0.031} \quad (2)$$

$$z_c = \frac{c - 2.9075}{0.026} \quad (3)$$

The degree of crystallization of GBP was determined by taking the ratio of the intensity of the peak diffracted by (32-2) plane of $(\text{RE})_5\text{Si}_4\text{Al}_2\text{O}_{17}\text{N}$ phase at 2θ value of $32,70^\circ$ and the intensity of the peak diffracted by (101) plane of β -SiAlON phase at 2θ value of $33,40^\circ$.

Microstructures of the as-sintered and as-oxidized samples were investigated by SEM (Zeiss-Supra 50VP) in back-scattered electron (BSE) mode, and the concentration of the elements in the content of oxidation products were analyzed by energy dispersive x-ray spectroscopy (EDX) which was attached to this SEM. The amount of GBP in as-sintered ceramics were visually determined by analyzing of SEM images with Image J analysis program.

3. RESULTS AND DISCUSSION

3.1. Microstructural characterization of as-sintered ceramics

Figure 1 (a) and (b) show the BSE-SEM images of Y-S and Er-S ceramics, respectively and (c) shows the XRD spectrum of these ceramics. While the dark gray elongated grains were β -SiAlON phase, α -SiAlON phase was observed as light gray equiaxed grains in the images. The GBP distributed through-out the microstructures homogeneously is seen as white small pockets due to their high atomic number RE concentration. Although the distribution of α and β -SiAlON grains in both microstructures are quite similar, the aspect ratio of β -SiAlON grains was seen slightly higher for Er-S sample (Fig 1 (a) and (b)). Moreover, a more bimodal distribution of β -SiAlON phase was detected for Er-doped sample since much finer β -SiAlON grains were formed in addition to the large elongated ones compared to Y-S. The bimodal distribution of β -SiAlON grains is an important indication of the material resistance against to crack propagation [11-13]. According to XRD spectrum given in Fig.1 (c), a crystalline GBP apart from α and β -SiAlON phases was formed in a stoichiometric formula of $(\text{RE})_5\text{Si}_4\text{Al}_2\text{O}_{17}\text{N}$. In Table 1, the amounts and degrees of crystallization of GBPs as well as β -SiAlON content and z values were summarized. It was seen that the main difference

between Y_2O_3 and Er_2O_3 was their effects on the crystallization behavior of GBP rather than α/β ratios, z values and/or GBP amounts. While the degree of GBP crystallization value of Y-S ceramic was calculated as 0.13, it was determined more than twice for Er-S ceramic due to a possible formation of liquid phase with lower viscosity during sintering as suggested by Hampshire and Pomeroy [18].

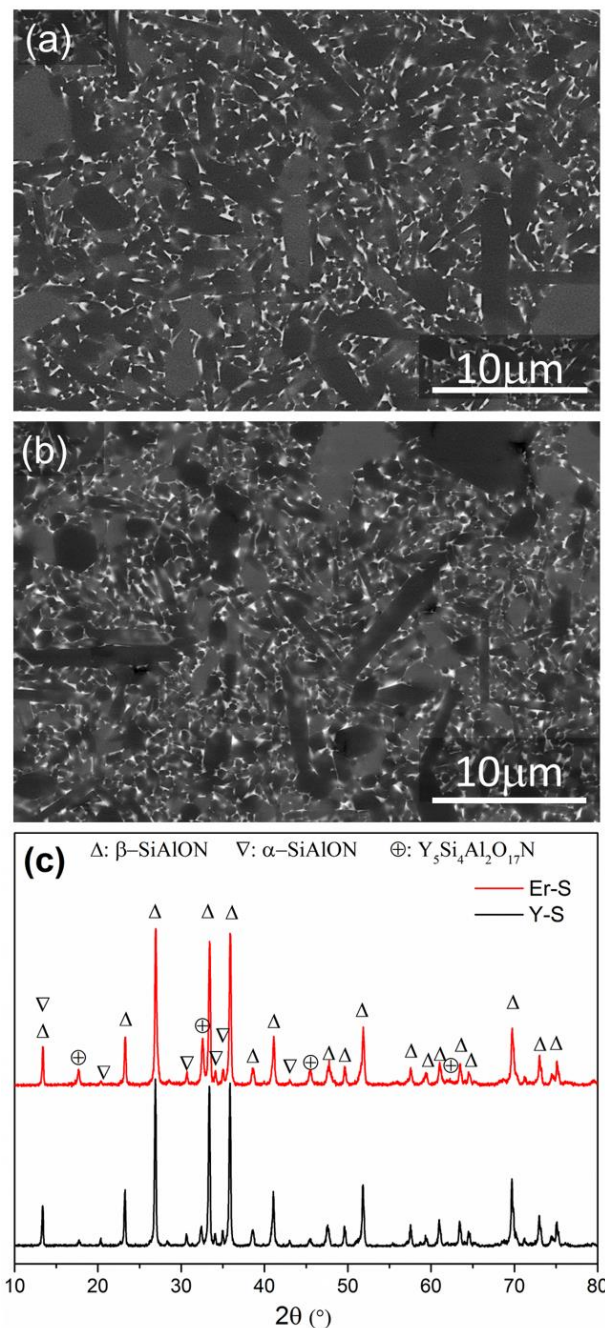


Figure 1. BSE-SEM images of as-sintered (a) Y-S ve (b) Er-S samples and (c) XRD spectrum of these compositions

Table 1. Phase properties of as-sintered Y-S ve Y-Er ceramics

	Y-S	Er-S
Dopant type	Y ₂ O ₃	Er ₂ O ₃
β/α (%)	86	86
z value of β-SiAlON (Si_{6-z}Al_zO_zN_{8-z})	1,06	1,02
Amount of GBP (vol.%)	8,13	7,73
Crystallization degree of GBP (I_{GBP}/I_{β-SiAlON})	0,13	0,34

3.2. Oxidation behavior of SiAlON compositions

3.2.1. Weight change

The oxidation behavior of Y and Er-doped SiAlON ceramics was examined by the weight change resulted by the oxidation reactions and a standard test method, the details of which was given in [14] and [15], was used to compare the oxidation resistance of these ceramics, quantitatively. Figure 2 shows the weight change curves ($\Delta m/m_0 \times 100$) of the Y-S and Er-S compositions as a function of oxidation temperature and the first order derivative of these curves ($d(\Delta m/m_0 \times 100)/dT$), which indicate the temperature at which the oxidation rate is maximum. It is clear in the graphs that while only a slight weight gain was observed at the temperature above 1250°C, the rate of weight gains due to oxidation reactions increased significantly above 1325°C for both Y-S and Er-S ceramics. While the tangent of weight gain curve for Y-S composition intersects the temperature axis (y-axis) at 1320°C, a slightly higher value was found for Er-S composition (1333°C) which indicated that the starting temperature of oxidation for Er-S sample was higher than that of Y-S sample. Although the starting oxidation temperature of Y-S was lower, the

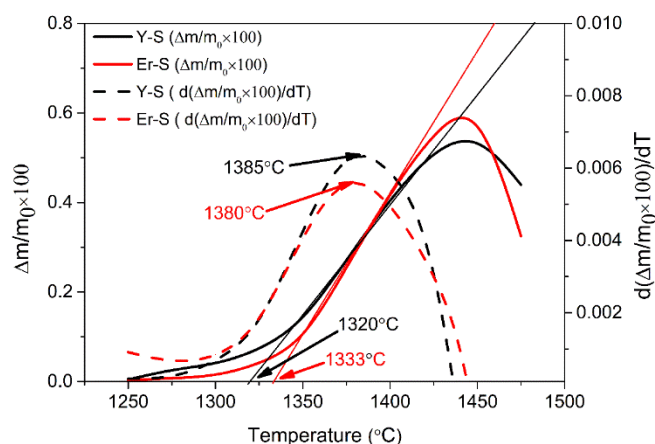


Figure 2. Weight change ($\Delta m/m_0 \times 100$) and derivative weight change ($d(\Delta m/m_0 \times 100)/dT$) curves of Y-S and Er-S ceramics as a function of oxidation temperature.

weight gain rate was also lower for this sample with increasing temperature due to its lower slope in comparison to Er-S composition. The maximum value of the slope shows the temperature at which the oxidation rate is the highest [14,15]. These temperatures were obtained from the peak of derivative curves and were found close to each other as 1385 and 1380°C for Y-S and Er-S compositions, respectively. At higher temperatures above this, the oxidation rate became slower and finally the samples started to lose weight due to evaporation of the gas products as a result of severe oxidation reactions.

3.2.2. Surface analysis

In Figure 3, micrographs of the surfaces of Y-S and Er-S ceramics after oxidation tests performed at 1250-1550°C with 100°C intervals. It was seen in Fig 3 (a) and (b) that white elongated crystals with a length of 3-5 μm formed throughout a dark gray matrix on the surface of the samples at 1250°C. The XRD analysis from the oxidized surfaces of the samples (Figure 4), showed that the elongated crystals and dark gray matrix are RE-silicates ((RE)₂Si₂O₇) and cristobalite (SiO₂), respectively. The formation of silicate crystals on the surface of SiAlON ceramics prepared by trivalent RE cations such as Y⁺³, Yb⁺³, Sm⁺³ was also reported in [8-10]. At 1350°C, a significant growth of the silicate crystals was observed and almost whole surface of the samples was covered by these crystals (Fig. 3 (c) and (d)).

Moreover, the amount of cristobalite phase increased at this temperature according to increase in the intensity of (111) plane of cristobalite peak at $2\theta \sim 21.6^\circ$ in Fig 4. While a significant formation of middle-like mullite phase (Al₆Si₂O₁₃) apart from silicate and cristobalite phases was detected for Y-S composition, a limited mullite formation was detected for Er-S sample. Crystallization of mullite from the melt which was rich in Si, Al and O atoms during oxidation is a common process for many SiAlON ceramics [16]. It is well known that highly dense oxide scale which contains cristobalite and mullite phases without any micro-cracks increases the oxidation resistance of the substrate by inhibiting the inward and outward diffusion of the atoms. In this case, however, some interconnected cracks on the oxide scale were started to form as seen in Fig. 3 (c) and (d). Furthermore, the silicate and aluminate crystals available on this oxide scale can also alter the chemical composition and therefore, protection capability of the oxide scale [8]. In order to explain the oxidation resistance of SiAlON ceramics as a function of RE elements used, ionic field strength (IFS) which is an indication of the interaction of cation with its surrounding atoms were generally used.

IFS, which was defined as the ratio of valance of a cation to square of its radius mathematically, proportional with the mechanical and chemical durability as well as high temperature resistance of the silicate phase [17]. For the silicate phases in this study containing Y⁺³ and Er⁺³ RE elements with the radii of 90 and 89 pm, respectively, the IFS values were calculated as 3,70 and 3,79 1/Å². It can be

concluded that similar oxidation resistance of the Y-S and Er-S compositions were observed by considering corresponding IFS values as well as maximum oxidation

temperatures obtained from weight change results as given in previous section.

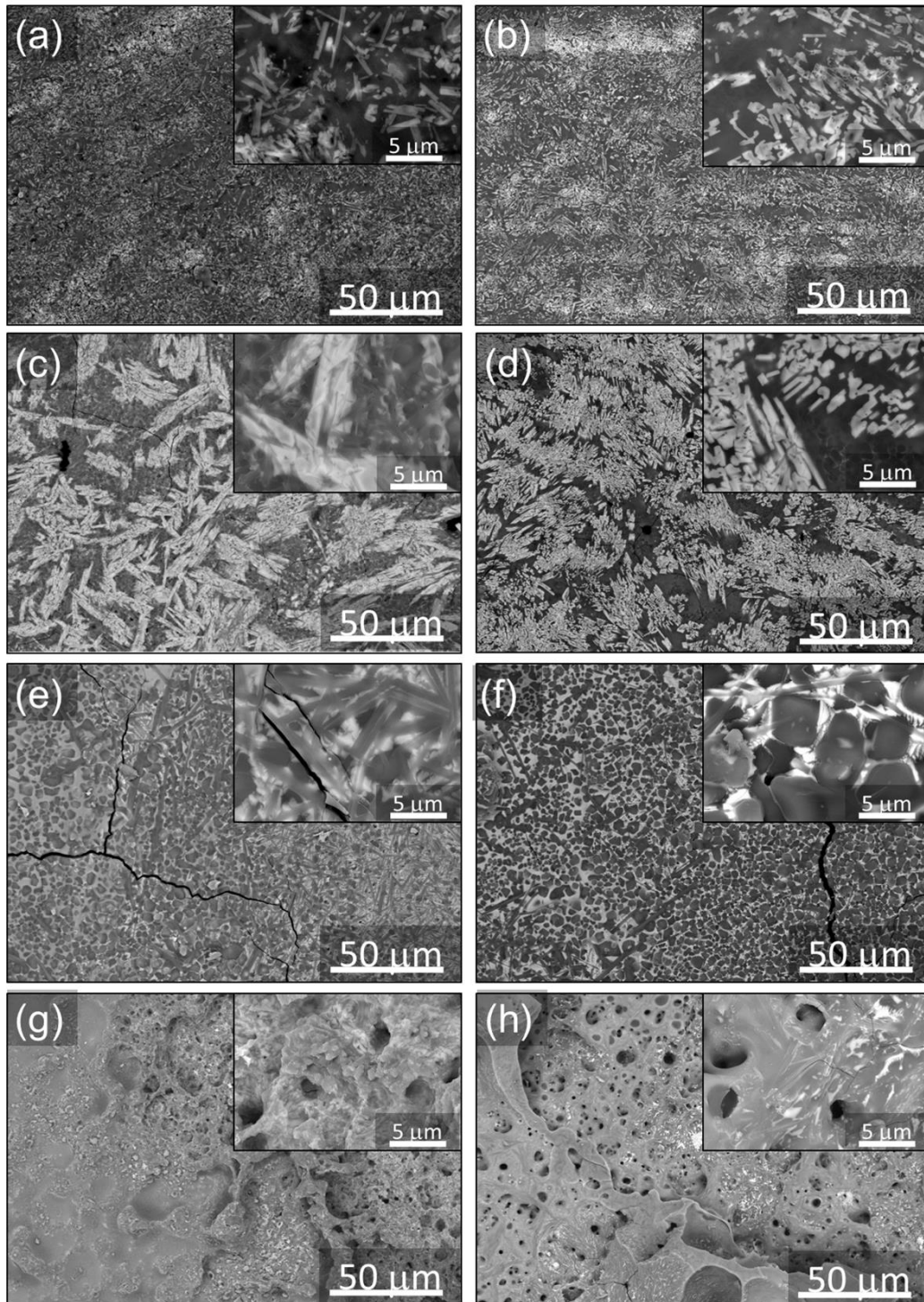


Figure 3. The surface BE-SEM images of Y-S and Er-S samples oxidized at (a) and (b) 1250°C, (c) and (d) 1350°C, (e) and (f) 1450°C and (g) and (h) 1550°C, respectively.

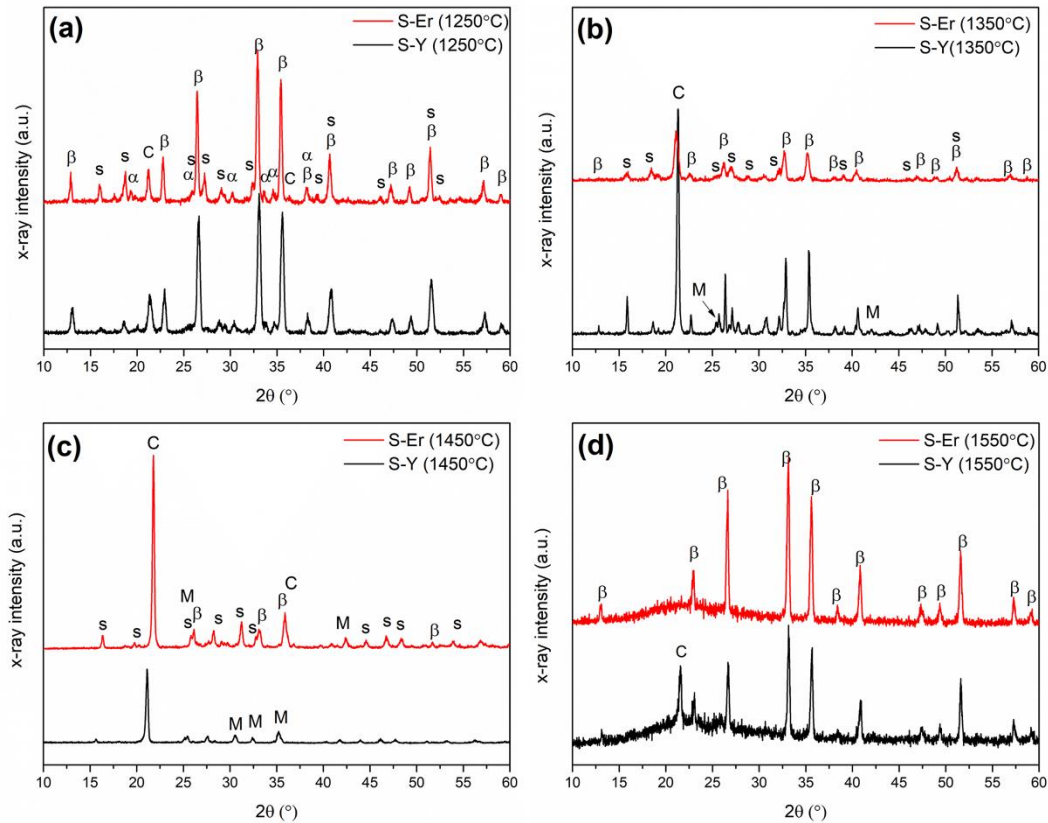


Figure 4. The XRD spectrum of surfaces of Y-S and Er-S samples oxidized at (a) 1250°C, (b) 1350°C, (c) 1450°C and (d) 1550°C

At above 1400°C, significant dissolution of dendritic silicate crystals into the melt due to a possible eutectic reaction at ~1400 was observed in accordance with Corapcioglu and Kurama [9]. It was clear that the oxidation rate of Y-S and Er-S samples increased above 1450°C due to increase in diffusion rates of Y and Er RE elements in SiO₂ based melt in comparison to that of in silicate crystals, and therefore, weight loss rather than weight gain was started to be observed. The melt showed high tendency to crystallize as cristobalite and mullite during cooling from oxidation temperature as seen in Fig. 4. Besides, it was obvious in micrographs and XRD patterns given in Fig 3 and Fig 4, respectively that a considerable silicate phase nucleation around the cristobalite and mullite grains occurred for Er-S composition in contrast to Y-doped sample in which the silicate nucleation was quite limited. When the oxidation temperature was 1550°C, some vapor products resulted by severe oxidation reactions were started to escape from the surfaces of the samples. Therefore, a porous morphology was obtained as illustrated in micrographs given in Fig. 3 (g) and (h). The XRD analysis given in Fig. 4 (d) also confirmed severe evaporation of the oxidation products from the surface due to significant increase in the peak intensities of SiAlON phases which were almost invisible at previous oxidation temperature (1450°C). While the oxide scale remained on the surface was totally amorphous for Er-S sample since no peaks were observed except β-SiAlON, a partial cristobalite crystallization was also detected for Y-S.

3.2.3. Cross-section analysis

The inward and outward diffusion of atoms takes place at high temperatures along the cross-section of the samples during oxidation process. In Figure 5, the cross-section SEM images of Y-S and Er-S samples which were oxidized at 1350°C, were given. It was seen that three distinguished regions were formed as the result of diffusion processes. The first region far from the surface is the main material which was not affected by the oxidation-based reactions. In the second region, a microstructure free of GBP due to partial/total diffusion of Al, Si, N, RE atoms in GBP towards to the surface of the samples was observed. While a complete diffusion of GBP which left a highly porous structure was seen for Y-S composition, higher density region due to partial diffusion of the GBP was occurred in case of Er-S sample. It was assumed that the diffusion rate of the elements directly dependent on the crystallization of the phases at the grain boundaries [9]. Consequently, slightly higher stability for Er-S composition was expected compared to Y-S due to its remarkable crystallization of GBP (Table 1). Besides the diffusion of the elements towards to surface which was derived by the chemical potential, the diffusion of oxygen in atmosphere from surface to inner regions and of nitrogen in SiAlON from inner parts to surface were also took place [8-10]. During oxidation process, a silicate melt, in which SiAlON grains rich in oxygen dissolved, was formed. When the concentration of RE elements in this silicate melt became

supersaturated, $(RE)_2Si_2O_7$ crystals started to nucleate in the oxide scale on the surface of the samples. Then, the concentration of RE elements in remained silicate phase became much lower and cristobalite and mullite

crystallization occurred from this silicate melt. The bubbles on the third layer (oxide layer) was created by the N_2 evaporation from this low viscosity oxide layer.

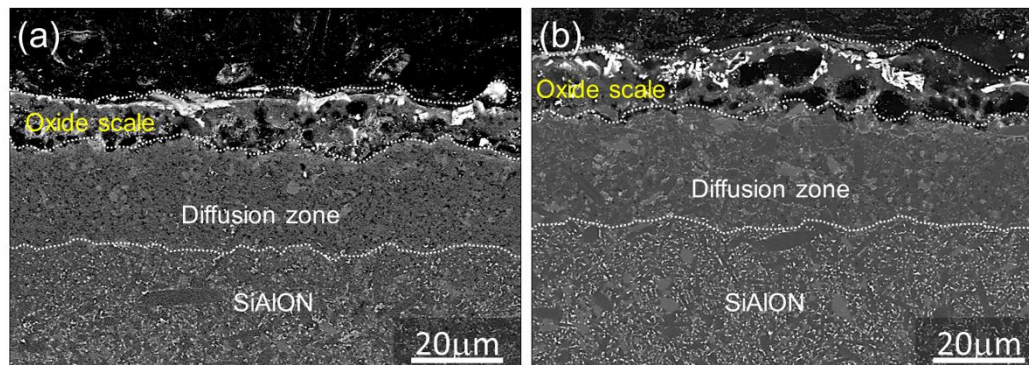


Figure 5. The cross-section micrographs of (a) Y-S and (b) Er-S ceramics oxidized at 1350°C.

4. CONCLUSIONS

The relative oxidation behavior of α/β -SiAlON ceramics prepared by Er_2O_3 and Y_2O_3 was investigated and the following results were obtained:

- 1) While the α/β -SiAlON ceramics doped with Y_2O_3 ve Er_2O_3 had similar microstructural properties, the crystallization of GBP in Er-S composition was found remarkably higher. However, the difference in GBP crystallization was not observed as highly effective parameter on oxidation resistance of these two samples. Only a small microstructural difference on diffusion zone was detected between these two compositions.
- 2) After oxidation tests performed at 1250-1550°C, a similar weight change was observed for both Y and Er-doped SiAlONs. The maximum oxidation temperatures for Y-S and Er-S compositions were pointed out as 1385 and 1380°C, respectively.
- 3) At 1250°C, the formation of silicate crystals as well as cristobalite phase were detected on the surface of the samples. The growth of these crystals with increasing temperature was also recorded. At 1450°C the silicate crystals were started to be dissolved in oxide melt, and a weight loss rather than weight gain were measured due to evaporation of gaseous products from the system.
- 4) During oxidation process, three distinct regions were observed at the cross-section of the samples. A porous structure was resulted in case of Y-S composition due to complete diffusion of GBP towards to the surface of the sample. The difference in structure of this zone was believed due to different crystallinity of the GBPs in as-sintered samples.

ACKNOWLEDGEMENTS

The author thanks to the Head of Materials Science and Engineering Department, Eskisehir Technical University for facilitating characterization experiments and MDA Co Inc. for kindly providing raw powders.

REFERENCES

- [1] D. Hardie and K. H. Jack, "Crystal structures of silicon nitride," *Nature*, vol. 180, no. 4581, pp. 332–333, 1957.
- [2] I. W. Chen and A. Rosenflanz, "A tough SiAlON ceramic based on α - Si_3N_4 with a whisker-like microstructure," *Nature*, vol. 389 (6652), pp. 701–704, 1997.
- [3] T. Ekström and M. Nygren, "SiAlON ceramics," *J. Am. Ceram. Soc.*, vol. 75, no. 2, pp. 259–276, 1992.
- [4] N. C. Acikbas, H. Yurdakul, H. Mandal, F. Kara, S. Turan, A. Kara, and B. Bitterlich, "Effect of sintering conditions and heat treatment on the properties, microstructure and machining performance of α - β -SiAlON ceramics," *J. Eur. Ceram. Soc.*, vol. 32, no. 7, 1321–1327, 2012.
- [5] A. Çelik, M. S. Alağaç, S. Turan, A. Kara, and F. Kara, "Wear Behavior of solid SiAlON milling tools during high speed milling of Inconel 718," *Wear*, vol. 378, pp. 58-67, 2017.
- [6] M. H. Lewis and P. Barnard, "Oxidation mechanisms in SiAlON ceramics," *J. Mater. Sci.*, vol. 15, no. 2, 443-448, 1980.
- [7] M. J. Pomeroy and S. Hampshire, "Oxidation processes in a high substitution β '-sialon," *Mater. Chem. Phys.*, vol. 13, no. 5, 437-448, 1985.
- [8] J. Yu, H. Du, R. Shuba and I. W. Chen, "Dopant-dependent oxidation behavior of α -SiAlON ceramics," *J. Mater. Sci.*, vol. 39, no. 15, pp. 4855-4860, 2004.

- [9] G. Corapcioglu and S. Kurama, "Oxidation behaviour and kinetics of α -SiAlON ceramics," *Mater. High Temp.*, vol. 26, no. 2, pp. 145-151, 2009.
- [10] L. O. Nordberg, M. Nygren, P. O. Käll and Z. Shen, "Stability and oxidation properties of RE- α -Sialon ceramics (RE= Y, Nd, Sm, Yb)," *J. Am. Ceram. Soc.*, vol. 81, no. 6, 1461-1470, 1998.
- [11] M. Zenotchkine, R. Shuba, J. S. Kim and I. W. Chen, "R-curve behavior of in-situ toughened α -SiAlON ceramics," *J. Am. Ceram. Soc.*, vol. 84, no. 4, 884-886, 2001.
- [12] E. Y. Sun, P. F. Becher, K. P. Plucknett, C. H. Hsueh, K. B. Alexander, S. B. Waters and M. E. Brito, "Microstructural design of silicon nitride with improved fracture toughness: II, effects of yttria and alumina additives," *J. Am. Ceram. Soc.*, vol. 81, no. 11, 2831-2840, 1998.
- [13] J. Kim, A. Rosenflanz and I. W. Chen, "Microstructure control of in-situ-toughened α -SiAlON Ceramics," *J. Am. Ceram. Soc.*, vol. 83, no. 7, 1819-1821, 2000.
- [14] X. T. Wang, Y. J. Zhang, X. Ling, P. Xiao, L. Lin., Q. Chen, J. Wang, S.W. Jia, W. M. Zhu, X. C. Zhu, F. Y. Ji, "Testing of the oxidation resistance of MgAlON materials with non-isothermal oxidation method," in *Proceedings of International Conference on Materials Science and Engineering Application (ICMSEA)*, April 21-23, Nanjing, China, 2017.
- [15] X. T. Wang, Y. Zhang, P. Xiao, B. Wang, L. Xu, L. Lin and J. Huang, "Characterization of the oxidation resistance property of SiAlON materials with the standard method of GB/T 32329-2015", in *Proceedings of 6th International Conference on Mechatronics, Materials, Biotechnology and Environment (ICMMBE 2016)*, August 13-14, Yinchuan, China, 2016.
- [16] W. D. Kingery, H. K. Bowen and D. R. Uhlmann, *Introduction to Ceramics*, Wiley, New York, 634-643, 1975
- [17] P. F. Becher, S. B. Waters, C. G. Westmoreland and L. Riester, "Compositional effects on the properties of Si-Al-RE-based oxynitride glasses (RE= La, Nd, Gd, Y, or Lu)," *J. Am. Ceram. Soc.*, vol. 85, no. 4, 897-902, 2002.
- [18] S. Hampshire and M. J. Pomeroy, "Grain boundary glasses in silicon nitride: a review of chemistry, properties and crystallization," *J. Eur. Ceram. Soc.*, vol. 32, no. 9, 1925-1932, 2012.